Adaptive Fixed-Time Consensus Protocol of a DC Microgrids Cluster

Zaid Hamid Abdulabbas Al-Tameemi, Tek Tjing Lie, R. Zamora
Department of Electrical and Electronic Engineering
Auckland University of Technology, New Zealand
email:zaid.altameemi@autuni.ac.nz, {tek.lie,
ramon.zamora}@aut.ac.nz

Frede Blaabjerg
Department of Energy Technology
Aalborg University, Denmark
email: fbl@et.aau.dk

***Abstract*— This article introduces the Adaptive Fixed-Time Consensus algorithm (AFTCA) using a saturation function to address challenges arising from the constant parameter values in different operational conditions. To enhance the cluster's adaptability during emergencies, an Artificial Neural Networks (ANN) technique is leveraged to predict these parameters. Implementing this technique in the secondary control layer improves both cluster convergence and bus voltage regulation. The proposed control method outperforms existing approaches in the literature, achieving swift current convergence and enhanced voltage recovery across diverse operating conditions. The performance of the proposed control method is evaluated by simulating a cluster of four DC microgrids (MGs) using MATLAB.**

Keywords DC Microgrid cluster; Voltage regulation, Current sharing, ANN, and AFTCA.

I. INTRODUCTION

Microgrids (MGs) are compact electrical networks comprising end-use loads, energy storage devices, and distributed generators (DGs) [1]. They facilitate localized grid development by integrating various renewable energy sources (RES) [2]. Literature highlights multiple MG topologies - AC, DC, and hybrid AC/DC - effectively combining RES with energy storage systems (ESS) to meet electricity demands [3]. Notably, the number of DC MGs is rapidly increasing, offering benefits such as simplified reactive power regulation, no synchronization requirements in standalone mode, and absence of harmonics or frequency compatibility issues compared to conventional AC MGs [4].

DC MGs face challenges, notably the reliability of power supply due to intermittent Renewable Energy Sources (RESs) like Photovoltaic (PV) and wind turbines (WT). Their generation heavily depends on weather conditions, causing power supply fluctuations and mismatches with load demand. A proposed solution involves deploying DC MG clusters to effectively address and overcome these challenges.

Clustered MGs offer substantial enhancements in flexibility and dependability [5]. They provide critical advantages, including (i) expanding renewable energy utilization and grid coverage, (ii) improving stability and reliability against generation uncertainty and demand fluctuations, and (iii) boosting overall operational efficiency, flexibility, and economic viability [5]. Effective coordination among these MGs is crucial to optimize resource utilization within the cluster and ensure maximal efficiency.

Prior studies have explored various control systems for efficient coordination of MGs within clusters, including centralized, decentralized, distributed, and hierarchical control. Among these, hierarchical control stands out for its notable coordinating abilities, comprising primary, secondary, and tertiary levels, each handling distinct tasks. Consensus protocols, particularly at the tertiary level, have been utilized in literature for data exchange coordination [6]-[8]. These protocols' convergence algorithms fall into categories such as linear, finite-time, and fixed-time convergence [9],[10],[11]. Linear consensus, favoured for its simplicity, is commonly adopted in distributed control and management of microgrids (DCMMGs) research [8],[12]. However, its suitability diminishes in complex communication topologies and emergency scenarios requiring rapid response and accurate monitoring within limited timeframes [10],[13].

Authors have proposed a finite-time consensus method in response to these challenges [10], [13], [14]. This approach ensures convergence within a predefined timeframe, making it more reliable for critical situations. It simplifies consensus establishment in limited steps, ensuring simultaneous agreement among all involved agents [15]. Demonstrating efficacy across operational scenarios, it outperforms linear consensus in terms of speed. However, it requires initial cluster conditions and a thorough understanding of the graph topology, which may vary and not always be readily available or precise. In contrast, the fixed-time consensus method offers accelerated convergence and a reliable assessment of convergence time independent of initial conditions [16], enhancing practicality in complex networks. Nonetheless, the optimal determination of control coefficients remains unresolved, potentially affecting convergence under critical circumstances. Hence, Artificial Neural Networks (ANNs) are employed to predict optimal control coefficient values based on cluster situations [17]. ANNs excel in handling complex, nonlinear data, providing more accurate predictions in high-dimensional and nonlinear environments [18], [19], [20]. Despite its complexity, this approach offers significant benefits in prediction accuracy and handling intricate data relationships, aligning with our objectives and challenges.

The main contributions of this study are listed as follows.

1. Implementation of a Fixed-Time Consensus Algorithm (FTCA) using a saturation function in the secondary control layer to limit control outputs, preventing cluster oscillations. This achieves faster current convergence and shorter settling times.
2. ANN technique is adopted in the paper to predict control coefficients of FTCA based on load change conditions in the cluster, which may enhance cluster response.

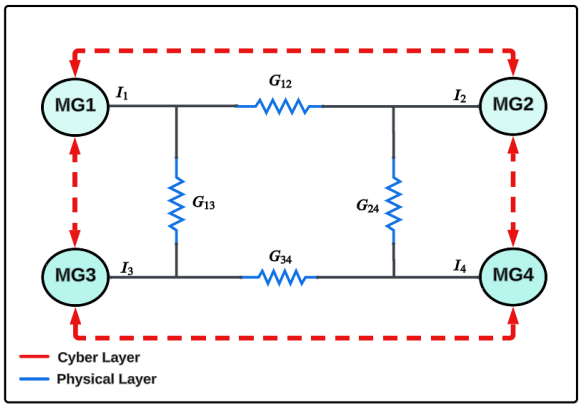

Fig.1. The configuration of DCMG Cluster.

II. PROBLEM FORMULATION

The DC MGs cluster, as shown in Fig. 1, comprises physical and cyber control layers. These layers facilitate efficient collaboration and coordination among MGs within the cluster. They are

instrumental in constructing a Laplacian matrix, representing the network architecture, and governing power transfer among MGs.

A. Physical Layer

The cluster's physical network can be embodied by an undirected weighted graph $Ge(\mathcal{V},\mathcal{E},w)$. The MGs and their power connections are deemed to be as nodes and edges, respectively. More specifically, $\mathcal{V}e=\{1,2,\dots,N\}$ is the index set of N MG, and $\mathcal{E}e \in \mathcal{V}\times\mathcal{V}$ is the edge set of coupled MGs in the cluster. These MGs are connected through conductance lines that represent the edge weights (w), which are assumed to *be* $1\Omega^{-1}$in the system. It is essential to mention that if an edge $(i,j)\in\mathcal{E}e$ implies the node, i can gather information from node j. $\mathcal{A}=[G_{ij}]\in R^{N\times N}$is the adjacency matrix along with non-negative elements, where $G_{ij}=1\Leftrightarrow if an\ edge\ (i,j)\in\mathcal{E}e$ and $G_{e_{ij}}=0$ otherwise .The Laplacian matrix $\mathcal{L}=[l_{ij}]\in R^{N\times N}$ is described as $l_{ij}=-g_{ij}, i\neq j$, and $l_{ii}=\sum_{j=1,j\neq i}^{N}G_{ij}$. It is necessary to mention that $\mathcal{D}=diag\{G_{11},G_{22},\dots,G_N\}$.

B. Cyber Layer

Graph theory can be considered as a graphical depiction of the communication networks among MGs in a cluster [7]. This subsection uses an undirected graph to describe the communication network topology amongst the MGs in the cluster. Considering a cluster consisting of a set of N interacting MGs. $Gc(\mathcal{V},\mathcal{E})$ is a weighted undirected graph, where $\mathcal{V}=\{1,2,\dots,N\}$ is the index set of N MGs and $\mathcal{E}\in\mathcal{V}\times\mathcal{V}$ is the edge set of coupled MGs. An edge $(i,j)\in\mathcal{E}$ indicates that node i can get data from node j. $\mathcal{A}=[a_{ij}]\in \boldsymbol{R}^{N\times N}$is the adjacency matrix with non-negative elements, where $a_{ij}=1\Leftrightarrow if\ edge\ (i,j)\in\mathcal{E}$and $a_{ij}=0$ otherwise. The Laplacian matrix $\mathcal{L}c=[l_{ij}]\in \boldsymbol{R}^{N\times N}$ is described as $l_{ij}=-a_{ij}, i\neq j$, and $l_{ii}=\sum_{j=1,j\neq i}^{N}a_{ij}$. It is crucial to mention that $\mathcal{D}=diag\{a_{11},a_{22},\dots,a_{NN}\}$.

III. The Main Control Objectives

Inspired by [21], the control objectives, including proportional current sharing and average voltage regulation, are derived for multiple MGs as expressed in Eq. (1) as follows.

$$\lim_{t\to\infty}\left(\frac{I_i}{I_{ci}}-\frac{I_j}{I_{cj}}\right)=0 \qquad \text{for all } i,j\in\mathcal{V}e \tag{1}$$

where $I_{ci}$and I_{cj}indicate the maximum capacities of MG_i and MG_j in cluster. These capacities need to be greater than zero. Eq. (2) is used to determine the overall average voltage of the cluster, which can be regulated to Vdcref in a steady state. In other words, $\bar{V}\mathrm{dc}-Vdc_{ref}$ should be Zero.

$$\bar{V}dc=\frac{1}{n}\sum_{i=1}^{n}Vdc_i=Vdc_{ref} \tag{2}$$

A. Adaptive fixed Time-Triggered Consensus Protocol

In this study, ANN is used to predict the control coefficients of the fixed time consensus algorithm, as shown in Fig.2. This approach is applied to multiple MGs, as shown in Eqs. (3) – (6):

$$V_{ref}=\Delta V_v+\Delta V_i \tag{3}$$

To produce the current correction factor, the error of the current (φc_i) needs can be expressed in Eq. (4) as follows:

$$\varphi_{Li}=a_{ij}\sum_{j\in i}\left(\frac{I_i}{I_{ci}}-\frac{I_j}{I_{cj}}\right)=0 \tag{4}$$

$$\varphi_{Li}=\sum_{j\in i}a_{ij}\frac{I_i}{I_{ci}}-\sum_{j\in i}a_{ij}\frac{I_j}{I_{cj}}=L_c\,I_c^{-1} \tag{5}$$

It is essential to mention that $[\mathcal{D}]-[\mathcal{A}]=L_c$; a_{ij} refers to the communication weight factor between $\mathrm{MG_i}$ and its close neighboring MGs in the cluster. To attain fast current convergence speed and less voltage recovery time, the secondary control layer in [21] is modified by using a fixed-time consensus algorithm based on the saturation function as expressed in Eq. (6).

$$u_i=k_1 sat(\varphi_{Li})^m+k_2 sat(\varphi_{Li})^n \tag{6}$$

where m , n , k_1 *and* k_2 indicate control coefficients that needs to be within a range of *1*. In this study, k_1 *and* k_2 are predicted by ANN based on load conditions in the cluster, as explained in the next section. By integrating the multiplication of Eq. (6) with the gain control (Ki), the current correction factor can be calculated in Eq. (7) as follows:

$$\Delta V_i=K_i\int_0^t u_i\,dt \tag{7}$$

the voltage error can be obtained by Eq. (8)

$$u_v=\bar{V}dc_i-Vdc_{ref} \tag{8}$$

The locally observed voltage regulation ($\bar{V}dc_i$can be determined by using Eq. (9), which depends on the local voltage of $\mathrm{MG_i}$ and integrating the multiplication of Eq. (6) with gain control (K_t) without needing the voltage information of $\mathrm{MG_j}$ which results in reducing communication between $\mathrm{MG_i}$ and its neighbors.

$$\bar{V}dc_i=Vdc_i+K_t\int_0^t u_i\,dt \tag{9}$$

where $K_t=K_i+K_v$; these control gains should be greater than zero. By substituting Eq.(9) into Eq. (8), the voltage error is expressed in Eq. (10).

$$u_v=(Vdc_i+K_t\int_0^t u_i\,dt)-Vdc_{ref} \tag{10}$$

From Eq. (10), the voltage correction factor is determined in Eq. (11) as follows.

$$\Delta V_v=K_v\int_0^t u_v dt=((Vdc_i+K_t\cdot k_1\int_0^t sat(\varphi_{Li})^m+sat(\varphi_{Li})^n\,dt)-Vdcref)\,K_v \tag{11}$$

$$V_{ref}=K_i\int_0^t u_i\,dt+K_v\int_0^t u_v\,dt \tag{12}$$

So, the combination of Eqs. (7) and (11) result in V_{ref} expressed in Eq. (12), which is transmitted to the primary control layer to correct the voltage mismatch caused by the droop control level. It is essential to mention that V_{ref} should be equal to $\mathrm{Vdc_i}$ at the steady state condition.

B. ANN implementation

ANNs are computational models inspired by the human brain's structure and function [22]. They excel in control systems, managing device behavior or system operations, typically in automation or signal processing contexts, offering high-speed, reliability, and robustness. ANNs' efficiency relies on weight adaptation within the network, ensuring optimal performance across layers [23]. In this study, 35000 simulated samples of load currents (I_{dc}) in the DC MGs cluster and control coefficients of fixed time consensus algorithm (k_1 *and* k_2), were collected from simulated cluster under varying load conditions to train ANN. These variables are essential as they directly impact the ANN's ability to simulate the relationship between changing load demands and necessary control adjustments for secure and effective cluster operation. The Levenberg-Marquardt algorithm was used for training, allocating 65% of data to learning, 15% to testing, and 15% to validation.

A feed-forward neural network was constructed in MATLAB with a single hidden layer of 10 neurons to model the relationship between input vector (load currents) and two associated target outputs (control coefficients). After training over 1,000 epochs to adjust weights and biases, the network's accuracy was evaluated by calculating the mean square error (MSE) between predicted and actual outputs. The model exhibited exceptional predictive ability across all datasets, with the MSE of the training set sharply decreasing and stabilizing at a very low value over increasing epochs, indicating effective learning [22], [23], as shown in Fig.3.

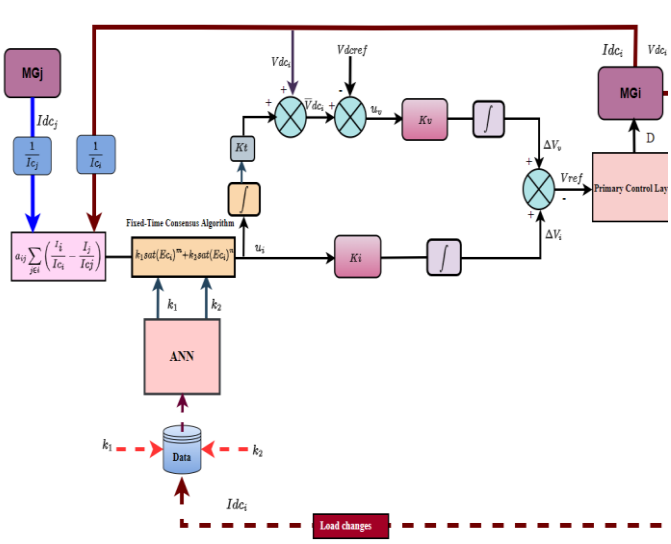

Fig.2 Proposed control scheme.

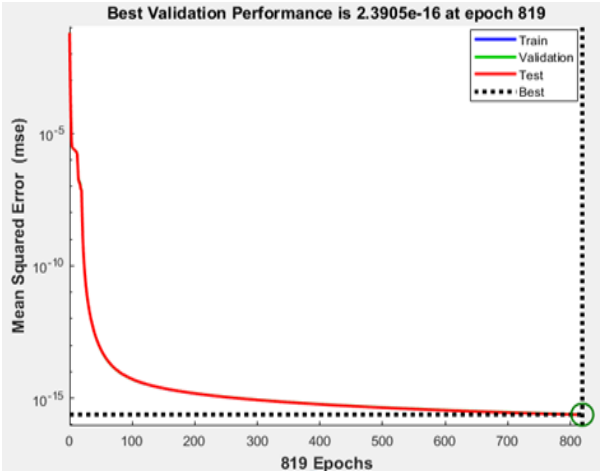

Fig.3 Best validation performance of ANN

III. RESULTS AND DISCUSSION

The MATLAB-simulated four DC-MGs cluster (depicted in Fig. 1) evaluates the proposed AFTCA's superiority over previous control methods. MGs are interconnected by tie lines, represented as 1-ohm resistances. Notably, each microgrid features two DG units in parallel, with DC-DC buck converters lowering the output voltage from 100V to 48V to match local loads. Fig. 3 outlines the key components of each DG, while Table 1 provides comprehensive data for each MG within the cluster.

$$\mathcal{L}_e = \begin{bmatrix} G_{11} & G_{12} & G_{13} & G_{14} \\ G_{21} & G_{22} & G_{23} & G_{24} \\ G_{31} & G_{32} & G_{33} & G_{34} \\ G_{41} & G_{42} & G_{43} & G_{44} \end{bmatrix} = \begin{bmatrix} 2 & -1 & -1 & 0 \\ -1 & 2 & 0 & -1 \\ -1 & 0 & 2 & -1 \\ 0 & -1 & -1 & 2 \end{bmatrix}$$

The local control layer, depicted in Fig. 4, is the primary control layer of the MG. It regulates the MG's voltage and current levels based on the reference voltage (V_{ref}) received from the global control layer, which includes secondary and tertiary control layers. The voltage loop adjusts the DG's output voltage and current based on measured and reference voltages, while the current loop adjusts the DG's output current based on measured and reference currents. These control loops enable the local control layer to achieve the MG's primary control objectives, ensuring stable output voltage and synchronized output power. This enhances overall stability, reliability, and efficient fulfilment of electrical power requirements within the MG.

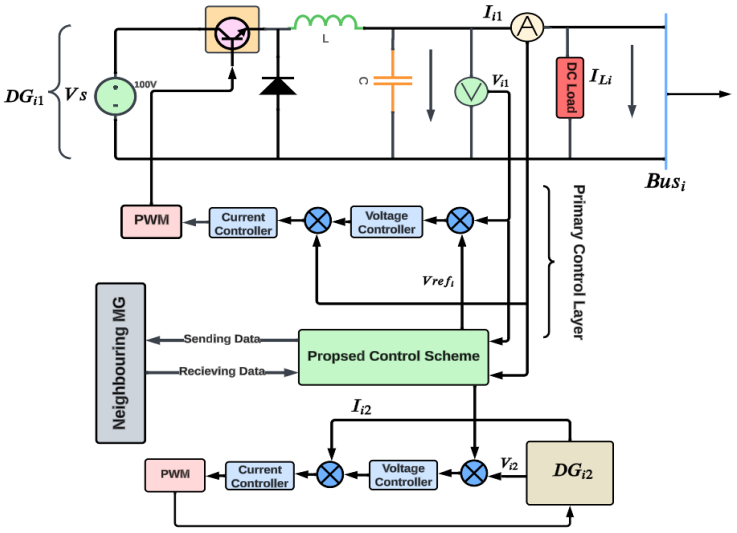

Fig. 4. The structure of each MG in the cluster.

Table1 MGs Parameters

Parameter	Value	Unit
Nominal Voltage	48	V
Converter Resistance	0.52	Ω
Converter Inductor	0.002	H
Converter Capacitor	0.005	F
Switching Frequency	20000	Hz
K_i and K_V	34	------
Conductance	1.25	------

For this study, the load resistances for each MG in the cluster have been adjusted to 24, 12, 16, and 9.6 Ω, with 48 V as the nominal voltage. Despite the loads being different, the load currents of the close-coupled MGs with identically rated currents (8A) and (10A) converge to their equilibrium setting point in 0.05s, which is deemed quite rapid in comparison to the [27] as demonstrated in Fig.5. It is discovered that the load currents converge to 3.1A, 3.1A, 3.9A, and 3.9A, confirming the strength of the proposed control technique in achieving accurate current allocation across the cluster's participant MGs, ensuring stability, efficiency, and reliability within the microgrid cluster. It also correlates to decreased power losses. In the following subsections, several scenarios are conducted to evaluate the efficiency of the proposed control mechanism under these circumstances.

A. Load changes

During the first scenario, the introduction of load resistances for the MGs at 1.5s and 2.5s resulted in an increase in the overall load current from 13.9A to 22.4A and subsequently to 28.4A. The observed results indicate a decrease in resistance ranging from 39% to 52.5% compared to the initial setup values. The system promptly adapted to the changes, as seen in Fig.5, by sustaining bus voltages at magnitudes of 48.2V, 48.6V, 47.5V, and 47.9V throughout the time interval of 2.5s to 3.5s. Additionally, the system demonstrated rapid convergence of load currents within a time frame of 0.025 seconds, namely throughout the interval of 0 to 1.5 seconds. Furthermore, the convergence of load currents after load changes at 1.5s and 2.5s occur within 0.015s and 0.002s, respectively, as indicated in Fig.6(a). This highlights the effectiveness of the proposed coordination method among the MGs inside the cluster.

In addition, it can be shown from Fig. 5(b) that the average bus voltages in the MG cluster stayed continuously within a narrow range of 47.86V to 48.0124V throughout periods of steady states. Moreover, the bus voltages quickly returned to normal values when disturbances occurred at 1.5s and 2.5s. Fig.5(c) demonstrates a negligible voltage tracking error, exhibiting less than 0.124 V and 0.06V variances for load changes lasting 1.5s and 2.5s, respectively. It is important to highlight that the main control objectives, as outlined in Eqs (4) and (8), have been successfully achieved, as seen in Figs. 5(c), 5(d), and 6(b).

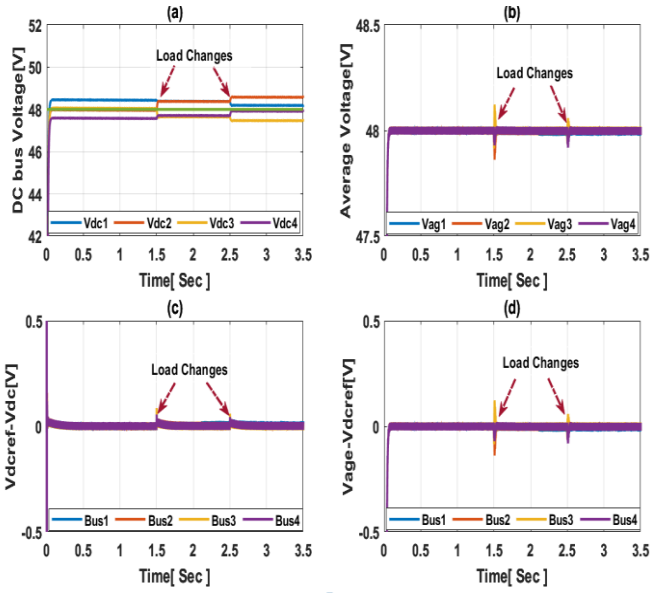

Fig.5. Scenario I (a) DC voltage, (b) Average voltage, (c) voltage regulation errors, and (d) Voltage observers (Eq. (8))

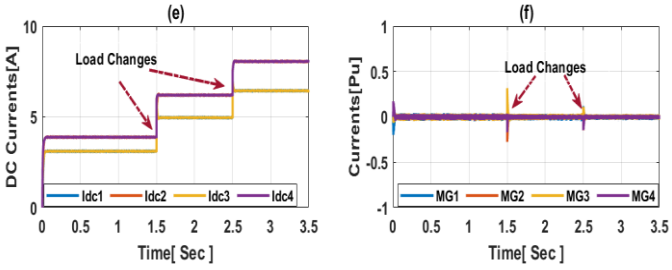

Fig.6. Scenario I (a) DC Current (b) Current Sharing errors (Eq. (4))

B. Abnormal conditions

The purpose of this scenario is to evaluate the cluster's performance under realistic situations by subjecting it to load changes and faults. In addition to the load changes mentioned in Subsection A, simulated faults were also implemented in MG2 and MG3 at 2s and 3s, respectively. Notwithstanding these interruptions, the system's stability is noticeable, as seen in Fig.7 (a), whereby the DC bus voltages persist within the specified limit. The convergence of load current occurs during the time interval of 0.001s to 0.04s, resulting in an accurate current sharing among the MGs involved, as seen in Fig.8(a). The cluster regularly exhibits average voltages ranging from 47.767V to 48.145V. Furthermore, the voltage tracking error of the buses remains within the range of 0.145V to -0.231V, as seen in Fig.7(c). The key control objectives, as defined in Eqs (4) and (8), have been effectively achieved, as seen in Figs. 7(d) and 8(b).

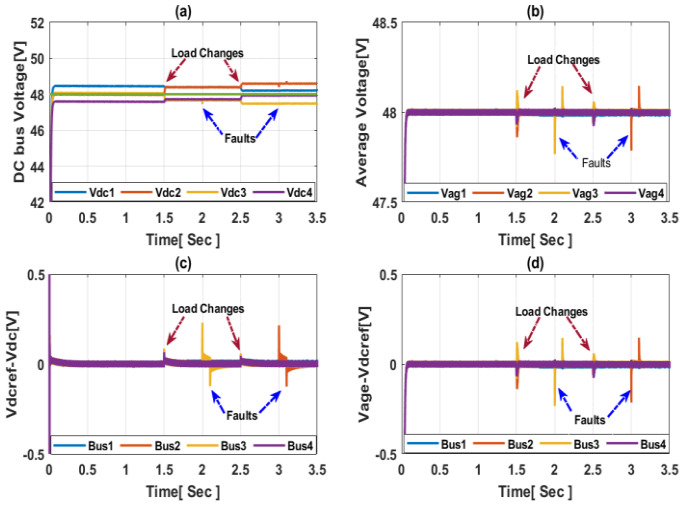

Fig.7. Scenario II (a) DC voltage (b) Average voltage (c) voltage regulation errors (d) Voltage observers (Eq. (8)).

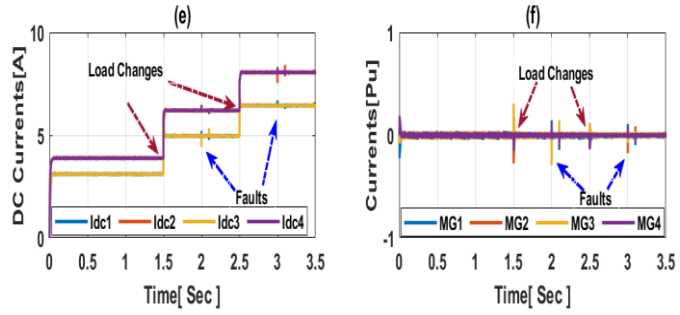

Fig.8. Scenario II (a) DC Current (b) Current Sharing errors (Eq. (4)).

V. COMPARISON WITH THE EXISTING CONTROL TECHNIQUES

This section investigates the impact of control coefficients on cluster performance with/without the use of ANN for coefficient prediction. Scenarios with random coefficient values were tested without ANN. It was found that decreasing these coefficients negatively affected load current convergence and DC voltage settling time, with the worst scenario achieving 0.22s and 0.22s, respectively (Fig.9(a)). Conversely, increasing coefficients improved load current convergence and DC voltage settling time to 0.13s and 0.2s, respectively. However, fixed coefficient values may hinder effective handling of load fluctuations in real-life scenarios.

In the case of using ANN, continuously determining coefficients reduced load current convergence and DC voltage settling time to 0.022s and 0.06s, respectively, enabling effective cluster response to load changes (Fig.9(b)). Additionally, this approach achieved better performance than [24], which attained load current convergence and settling times within 0.1s and 0.2s, respectively. These findings highlight the vulnerability of clusters with constant coefficient values to unpredicted load changes, a limitation addressed in this study.

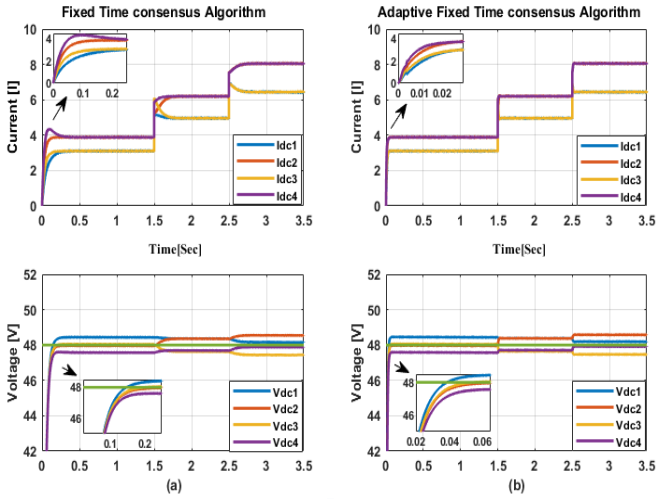

Fig.8 Currents convergence and Settling time of dc voltages (a) fixed-time consensus algorithm (b) adaptive fixed-time consensus algorithm.

VI. CONCLUSION

This article presents an AFTCA based on ANN for enhancing the performance of the secondary control layer in a cluster of four DC MGs (as shown in Fig.1). The feasibility of this control approach is demonstrated under various perturbative scenarios, including load variations and faults.

Key findings reveal that the DC voltages within the MG cluster consistently remain within predefined limits. Additionally, this method facilitates rapid cluster voltage restoration, ensuring accurate proportional current sharing based on the maximum ratings of the MGs. The average voltage observers exhibit quick and reliable convergence to the reference voltage, even in abnormal situations. Simulation results underscore the cluster's resilience to disruptions, thereby reinforcing the efficacy of the proposed control algorithm.

ACKNOWLEDGEMENT

The authors would like to thank Al-Furat Al-Awsat Technical University for their financial support to conduct this research. They would also like to note that this study is a part of the MBIE SSIF AETP program entitled Future Architecture of the Network.

REFERENCES

[1] Q. Xu, Y. Xu, Z. Xu, L. Xie, and F. Blaabjerg, "A Hierarchically Coordinated Operation and Control Scheme for DC Microgrid Clusters under Uncertainty," *IEEE Trans Sustain Energy*, vol. 12, no. 1, 2021, doi: 10.1109/TSTE.2020.2991096.

[2] M. Glinkowski *et al.*, "Microgrids," *Smart Grids: Clouds, Communications, Open Source, and Automation*, pp. 213–249, 2017, doi: 10.1201/b16908.

[3] O. Rezaei, O. Mirzapour, M. Panahazari, and H. Gholami, "Hybrid AC/DC Provisional Microgrid Planning Model Considering Converter Aging," *Electricity*, vol. 3, no. 2, pp. 236–250, Jun. 2022, doi: 10.3390/electricity3020014.

[4] S. K. Sahoo, A. K. Sinha, and N. K. Kishore, "Control Techniques in AC, DC, and Hybrid AC-DC Microgrid: A Review," *IEEE Journal of Emerging and Selected Topics in Power Electronics*, vol. 6, no. 2. 2018. doi: 10.1109/JESTPE.2017.2786588.

[5] Y. Han *et al.*, "Coordinated power control with virtual inertia for fuel cell-based DC microgrids cluster," *Int J Hydrogen Energy*, vol. 44, no. 46, 2019, doi: 10.1016/j.ijhydene.2019.06.128.

[6] A. Abhishek, S. Devassy, S. A. Akbar, and B. Singh, "Consensus Algorithm based Two-Level Control Design for a DC Microgrid," in *2020 IEEE International Conference on Power Electronics, Smart Grid and Renewable Energy, PESGRE 2020*, 2020. doi: 10.1109/PESGRE45664.2020.9070734.

[7] S. Moayedi and A. Davoudi, "Distributed Tertiary Control of DC Microgrid Clusters," *IEEE Trans Power Electron*, vol. 31, no. 2, 2016, doi: 10.1109/TPEL.2015.2424672.

[8] C. Wu, X. Hou, Y. Wang, X. Chen, and C. Liao, "SOC-featured Distributed Tertiary Control for Energy Management in DC Microgrid Clusters," in *2019 22nd International Conference on Electrical Machines and Systems, ICEMS 2019*, 2019. doi: 10.1109/ICEMS.2019.8922431.

[9] Q. Shafiee, T. Dragičević, J. C. Vasquez, and J. M. Guerrero, "Hierarchical control for multiple DC-microgrids clusters," *IEEE Transactions on Energy Conversion*, vol. 29, no. 4, 2014, doi: 10.1109/TEC.2014.2362191.

[10] M. Zaery, P. Wang, W. Wang, and D. Xu, "Distributed Finite-Time Controller for Economic Operation of DC Multi-Microgrids," in *IECON Proceedings (Industrial Electronics Conference)*, 2019. doi: 10.1109/IECON.2019.8926723.

[11] S. Sahoo, S. Mishra, S. M. Fazeli, F. Li, and T. Dragicevic, "A Distributed fixed-Time secondary controller for dc microgrid clusters," *IEEE Transactions on Energy Conversion*, vol. 34, no. 4, 2019, doi: 10.1109/TEC.2019.2934905.

[12] Q. Shafiee, T. Dragicevic, F. Andrade, J. C. Vasquez, and J. M. Guerrero, "Distributed consensus-based control of multiple DC-microgrids clusters," in *IECON Proceedings (Industrial Electronics Conference)*, 2014. doi: 10.1109/IECON.2014.7048785.

[13] Y. Li, P. Dong, M. Liu, and G. Yang, "A distributed coordination control based on finite-time consensus algorithm for a cluster of dc microgrids," *IEEE Transactions on Power Systems*, vol. 34, no. 3, 2019, doi: 10.1109/TPWRS.2018.2878769.

[14] Y. Li and P. Dong, "A distributed control based on finite-time consensus algorithm for the cluster of DC microgrids," in *2018 International Conference on Power System Technology, POWERCON 2018 - Proceedings*, 2019. doi: 10.1109/POWERCON.2018.8602262.

[15] F. Guo, C. Wen, J. Mao, and Y. D. Song, "Distributed Economic Dispatch for Smart Grids with Random Wind Power," *IEEE Trans Smart Grid*, vol. 7, no. 3, 2016, doi: 10.1109/TSG.2015.2434831.

[16] M. Zaery, P. Wang, W. Wang, and D. Xu, "A novel fully distributed fixed-time optimal dispatch of DC multi-microgrids," *International Journal of Electrical Power and Energy Systems*, vol. 129, 2021, doi: 10.1016/j.ijepes.2021.106792.

[17] I. A. Basheer and M. Hajmeer, "Artificial neural networks: Fundamentals, computing, design, and application," *J Microbiol Methods*, vol. 43, no. 1, 2000, doi: 10.1016/S0167-7012(00)00201-3.

[18] M. A. Millán, R. Galindo, and A. Alencar, "Application of Artificial Neural Networks for Predicting the Bearing Capacity of Shallow Foundations on Rock Masses," *Rock Mech Rock Eng*, vol. 54, no. 9, 2021, doi: 10.1007/s00603-021-02549-1.

[19] O. I. Abiodun, A. Jantan, A. E. Omolara, K. V. Dada, N. A. E. Mohamed, and H. Arshad, "State-of-the-art in artificial neural network applications: A survey," *Heliyon*, vol. 4, no. 11. 2018. doi: 10.1016/j.heliyon.2018.e00938.

[20] U. Ewuzie, O. P. Bolade, and A. O. Egbedina, "Application of deep learning and machine learning methods in water quality modeling and prediction: a review," in *Current Trends and Advances in Computer-Aided Intelligent Environmental Data Engineering*, 2022. doi: 10.1016/b978-0-323-85597-6.00020-3.

[21] J. Peng, B. Fan, Q. Yang, and W. Liu, "Distributed event-triggered control of dc microgrids," *IEEE Syst J*, vol. 15, no. 2, 2021, doi: 10.1109/JSYST.2020.2994532.

[22] T. Praveen Kumar, N. Subrahmanyam, and M. Sydulu, "CMBSNN for Power Flow Management of the Hybrid Renewable Energy–Storage System-Based Distribution Generation," *IETE Technical Review (Institution of Electronics and Telecommunication Engineers, India)*, vol. 36, no. 3, 2019, doi: 10.1080/02564602.2018.1465860.

[23] P. Singh and J. S. Lather, "Accurate power-sharing, voltage regulation, and SOC regulation for LVDC microgrid with hybrid energy storage system using artificial neural network," *Int J Green Energy*, vol. 17, no. 12, pp. 756–769, 2020, doi: 10.1080/15435075.2020.1798767.

[24] P. Wang, R. Huang, M. Zaery, W. Wang, and D. Xu, "A Fully Distributed Fixed-Time Secondary Controller for DC Microgrids," *IEEE Trans Ind Appl*, vol. 56, no. 6, 2020, doi: 10.1109/TIA.2020.3016284.